

Predicting the location and size of an explosive device detonated in an urban environment using evidence from building damage

B. M. Luccioni, R. D. Ambrosini and R. F. Danesi

This paper describes the determination of the mass of explosive and the location of the source of the explosion in a terrorist attack in a congested urban environment. A computational dynamic analysis was carried out for a real congested urban environment that corresponds to opposite rows of blocks of buildings in the same street. Many combinations corresponding to different locations and explosive masses were simulated, and the corresponding distributions of pressure and impulse on the building façades were obtained. Additionally, conclusions about the applicability of empirical expressions for evaluating incident and reflected pressure and associated impulses in a congested urban environment arise from a comparison with the numerical results, and are discussed in the paper. The structural damage produced by an explosion can be assessed with the use of isodamage curves, which approximately relate pressures and impulses to the damage produced in different types of building and parts of them. In general, isodamage curves have been obtained from a vast compilation of damage produced in masonry houses and other buildings and structural members, in both experimental and actual explosions. Damage contours were defined and used in order to compare the real damage with that obtained by the numerical simulation over a wide zone around the origin of the explosion. Additionally, conclusions that lead to the ability to discard many combinations of mass of explosive and location of the source of the explosion arise from the comparison of real and simulated damages, and are discussed in the paper.

1. INTRODUCTION

As a result of both accidental and intentional events in connection with important structures all over the world, explosive loads have received considerable attention in recent years. The activity related to terrorist attacks has increased, and, unfortunately, the present tendency suggests that it will be even larger in the future. This paper is concerned with the dynamic loading produced by the detonation of high-explosive materials in urban environments, a situation likely in a significant number of terrorist attacks.

When the attack has already occurred, it is very important to determine the location of the explosion and the mass of the explosive used. A useful tool in order to achieve this objective is the evidence of the crater generated by the explosion. However, if the bomb is in a vehicle and not in contact with the road, there may be little evidence of any cratering. Moreover, sometimes parts of the buildings collapse directly into the street, and it is almost impossible to reconstruct the crater. In other cases, the focus of the explosion is located inside a building at the ground floor above a lower stage in the subsoil, and no crater is formed. On the other hand, the mass of explosive obtained from crater dimensions has a significant spread. Some empirical expressions^{1,2} for crater dimensions can be found in the specialised literature, but, according to Kinney and Graham,¹ the results have a coefficient of variation of 30%.

In all the cases mentioned above, the use of computational analysis to evaluate the pressures and impulses generated by the detonation, and comparison with real damage registered in the urban environment, constitutes an attractive alternative for determining the location of the explosion and the mass of the explosive. Many combinations of locations and explosive mass can be simulated, and the corresponding simulated damage can be obtained from comparison with isodamage curves. Finally, the damage obtained must be compared with real damage. This makes it possible to discard most of the combinations simulated and obtain the most probable location and explosive mass used.

The above methodology is described and applied to a real damage scenario in this paper.

2. PROBLEM DESCRIPTION

To apply the methodology proposed in this paper, the entire affected zone should be inspected in considerable detail. Trained engineers and technicians should make this visual inspection, having in mind the levels defined in the isodamage curves to be used in the analysis. In addition to structural inspection it is also important to determine the area of window breakage, because, although glass presents a significant spread in its failure load, the lower limits can be used to discount any false combinations of explosive mass and location of charge.

The result of this stage of the analysis could be efficiently presented in condensed form by means of charts or damage contours.

In order to describe the methodology used to determine the charge location and explosive mass used in terrorist attacks, an actual explosion in a congested urban environment in the city of Buenos Aires will be analysed. The damage scenario is presented in Figs 1 and 2, and summarised in Fig. 3, which shows the rows of buildings of a block, on opposite sides of the same street.

The average damage in the building façades is presented with damage contours in Fig. 1, and can be summarised as follows:

- (a) front part of reinforced concrete building 1 completely destroyed
- (b) masonry building 3 (Fig. 3(a)) partially collapsed.
- (c) buildings 7 (Fig. 3(a)) with half of masonry façades in the direction of the street cracked
- (d) building 2 (Fig. 3(a)) with damage to masonry close to the target
- (e) buildings 4 and 5 (Fig. 3(b)) with external brickwork destroyed and damage in reinforced concrete structure up to storey five
- (f) glass broken in the entire block.

In many real situations the target of the attack can be easily recognised. In the situation analysed in this paper the building denoted as 1 in Fig. 3(a) was the target of the attack.

3. ASSESSMENT OF LOADING

3.1. Combinations analysed

As described above, many combinations of mass of explosive and location of the origin of the explosion were analysed.

The explosive mass was taken as 200, 300, 400 and 500 kg of TNT, and seven possible locations of the explosive charge were considered (see Fig. 4 and Table 1).

Taking into account the damage scenario presented in Fig. 3, all locations were selected in correspondence with the front



(a)



(b)

Fig. 2. Damage scenario: (a) row of buildings on the opposite side of the street to the target building; (b) buildings in front of the target building

of the target building, and are proved to be enough for defining the more probable location of the explosive in this case.

The range of explosive masses used in terrorist attacks is discussed in some papers,^{3,4} and is strongly dependent on how the explosive is supposed to have been transported. In actual situations there are often many other data that allow one to estimate the lower and upper limits for the explosive mass range to be considered. The range of explosive loads studied in this paper is in the medium range used in terrorist attacks on buildings, and it is later proved to be appropriate in this case. However, it could be necessary to extend this range to achieve the real quantity in other cases.

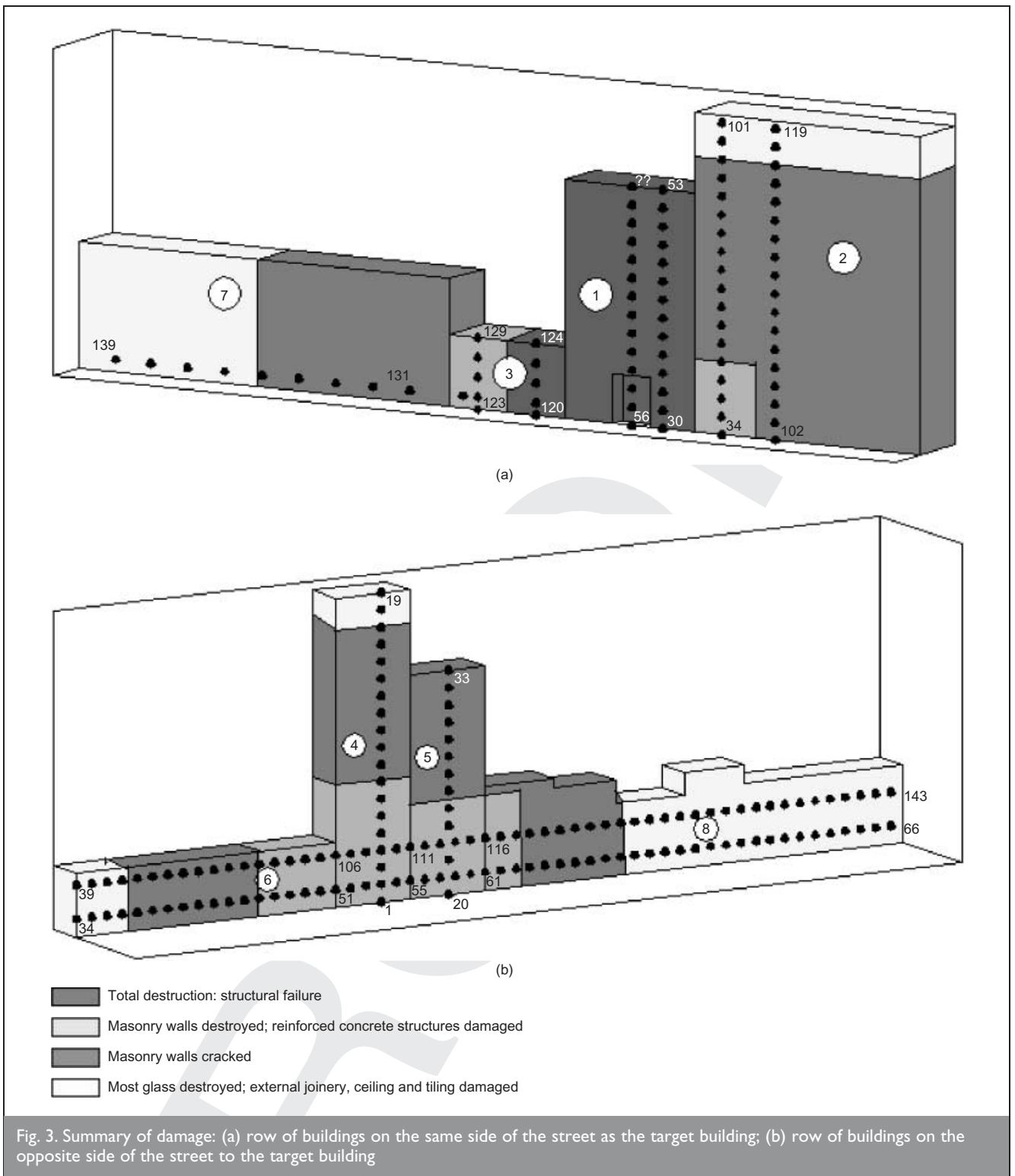


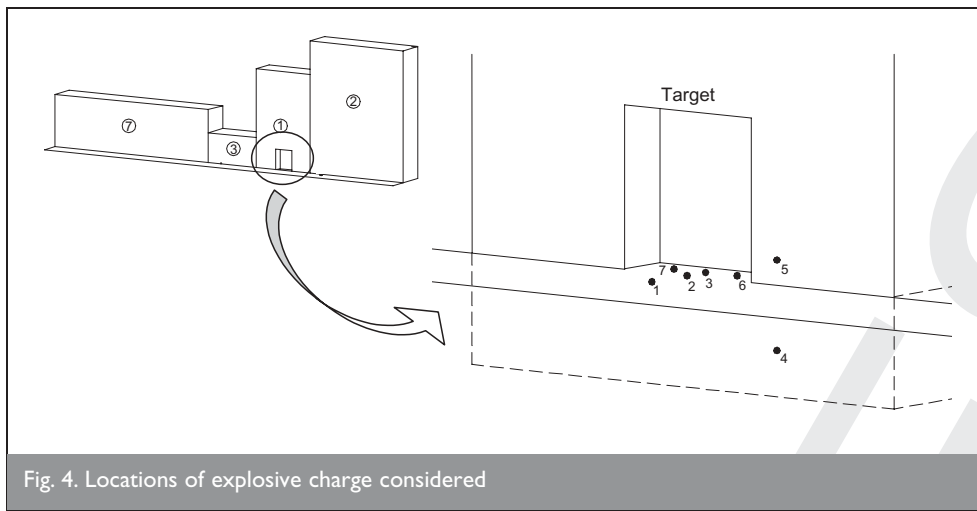
Fig. 3. Summary of damage: (a) row of buildings on the same side of the street as the target building; (b) row of buildings on the opposite side of the street to the target building

3.2. Generation of blast loading

Assuming that an initially spherically symmetric expanding blast wave encounters a series of obstacles, which subsequently create a complex three-dimensional flow field, the entire geometry can be modelled as three-dimensional from the start of the analysis. However, the number of cells required to achieve acceptable levels of accuracy in the initial phases of the calculation would be excessive. Alternatively, the use of symmetry conditions allows the spherical portion of the blast wave expansion to be represented by a one-dimensional, spherically symmetric model. This is achieved by a one-dimensional (1D) mesh using axial symmetry in AUTODYN-

2D.⁵ The number of cells required to produce accurate solutions is greatly reduced when compared with a full 3D model. When the spherical blast wave begins to interact with obstacles, the flow becomes multi-dimensional. However, before this time the 1D solution can be imposed, or remapped, onto a specific region of the multi-dimensional model. The 3D calculation can then proceed from that point. This procedure not only reduces the time required for a calculation but also increases its accuracy, thanks to the fine 1D mesh resolution in the initial high explosive detonation and expansion phases.

According to these considerations, the case under consideration



wave to continue 'through' the physical boundary of the model without reflection was considered for the rest of the boundaries.

It is clear that the splitting of the problem into Models 1 and 2 does not affect the results obtained in the row of buildings of the target building (Model 1). The lost wave reflections on the façades of the buildings of the opposite side of the street are considerably out of phase with respect to the main

shock, because of to the relatively long distances involved. However, on the opposite side of the street (Model 2), the situation is different. The coupling between the waves generated by the main shock and those due to the reflection on the target building are important. For this reason, the façade of the building was incorporated in Model 2.

In order to analyse the pressures and impulses generated on the façades of the buildings by the different combinations considered, many target points were defined in the models, and are indicated in Fig. 3. The principal variables of the analysis were recorded at these points.

Location	
1	2 m out of construction line. Central axis
2	Construction line. Central axis
3	1 m inside the entrance. Central axis
4	Subsoil. Central axis
5	5 m inside the target building. 5 m from construction line. Central axis
6	1 m inside the entrance. 1.25 m left
7	1 m inside the entrance. 1.25 m right

Table 1. Explosive locations considered

is divided into two stages. The initial detonation and expansion of the sphere of high explosive is modelled in a 1D, spherically symmetric model of 1 m radius with a Jones–Wilkins–Lee equation of state. The 1D expansion analysis continues until just prior to impingement of the blast wave on the rigid surface. At this time a 1D remap file is created, which is then imported into a three-dimensional model, allowing the reflection of the blast wave off the ground to be modelled.

The TNT material data available in material libraries⁵ were employed for this analysis.

In order to illustrate the initial expansion of the explosive, a remap to a 2D model was carried out, and the mesh and the velocity field after 0.07 ms are shown in Fig. 5.

3.3. Propagation of the blast wave

In view of the large number of degrees of freedom involved in one square model, the urban environment presented in Fig. 3 is subdivided in two models: Model 1 corresponds to the row of buildings where the target building is located, and Model 2 corresponds to the row of building on the opposite side of the street. The air in the two models was divided respectively into 380 000 and 615 000 cubic cells of 50 cm side.

The models were solved with a Euler formulation in which the nodes are fixed and the material (air) flows. To improve accuracy and efficiency, the FCT (flux corrected transport) algorithm implemented in AUTODYN⁵ was used. The buildings and the ground were considered to behave as rigid surfaces. A *transmit* boundary condition that allows a stress or pressure

3.4. Results of the numerical simulation

The propagation of the pressure wave on one side of the street obtained for one of the combinations analysed (300 kg TNT in location 2) is shown in Fig. 6. It can be seen that the stress wave starts with symmetry and regularity. However, multiple blast wave reflections in the buildings and soil lead to a complicated and unsymmetrical blast wave pattern.

In order to illustrate the results obtained, two curves representing the time history of the pressures and impulses for 300 kg TNT in location 2 are presented in Fig. 7. These records correspond to target point 4 located on the façade of building 4

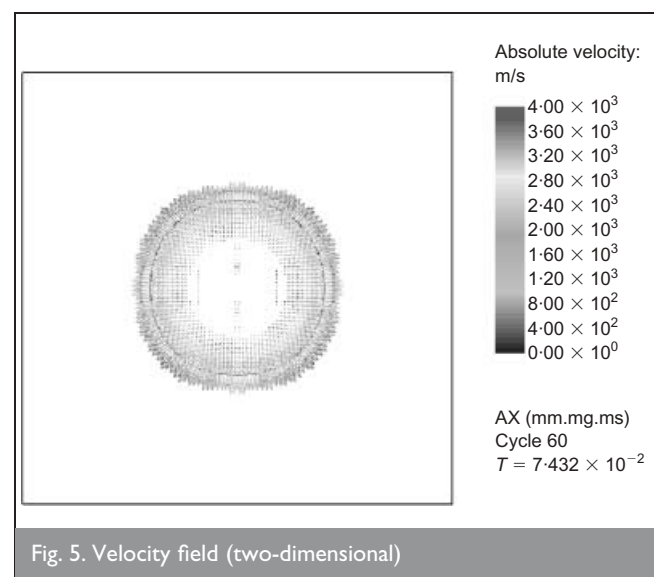


Fig. 5. Velocity field (two-dimensional)

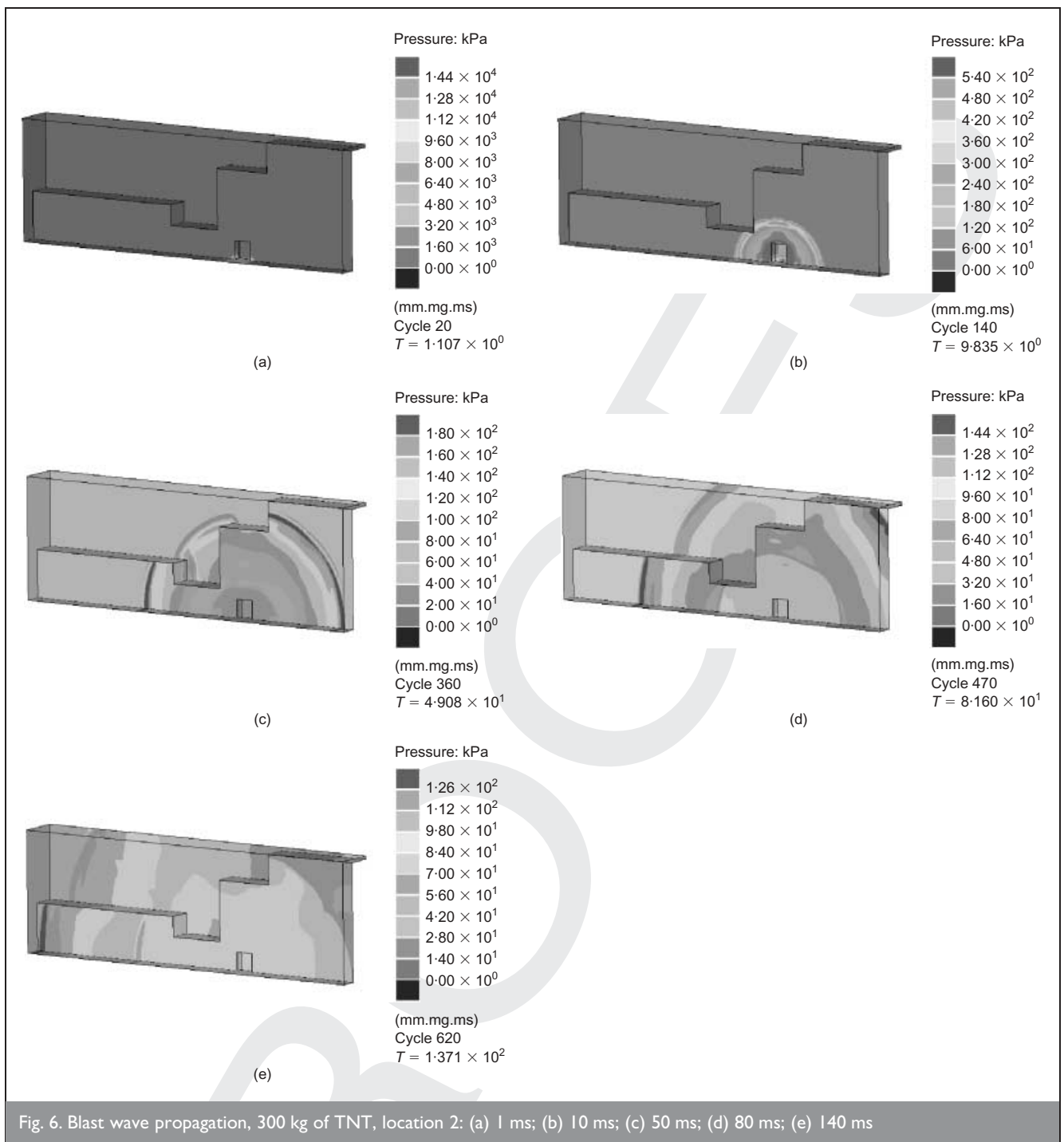


Fig. 6. Blast wave propagation, 300 kg of TNT, location 2: (a) 1 ms; (b) 10 ms; (c) 50 ms; (d) 80 ms; (e) 140 ms

(see Fig. 3(b)). The values of pressure and impulse presented correspond to reflected values.

The distribution of peak overpressure along the path of the target building, 1 m above the floor level, is presented in Fig. 8. As illustration, the values of peak overpressures obtained with empirical relations¹ for the same situation are also presented in Fig. 8. Fig. 8(a) shows clearly the result of neglecting reflections and the 'mach effect' of the blast wave. Moreover, the well-known limitations of empirical relations in the near field⁶ can be clearly observed in Fig. 8(b).

Additionally, the distribution of peak reflected overpressures and impulses with height for building 4, for the different combinations simulated, is presented in Fig. 9. The results on the façade of this building were chosen for this analysis

because they are more sensible to the difference of blast load location and charge than the other buildings. It can be seen that, because of the well-known cubic root law,⁷ the values of peak overpressure and impulse are more sensible to the location of the explosive than to its mass. When the focus of the explosion is moved away from the building analysed, the value of peak overpressure and impulse reduces until a certain limit when the pressure begins to increase owing to the effects of reflections of the blast wave on the façades of the buildings on the opposite side of the street. These results could never have been achieved through empirical expressions.

It may be recognised that the assumption that the façades of the buildings are rigid surfaces constitutes a limitation of this methodology, as it leads to an overestimation of pressures and impulses. In fact, part of the energy generated by the explosion

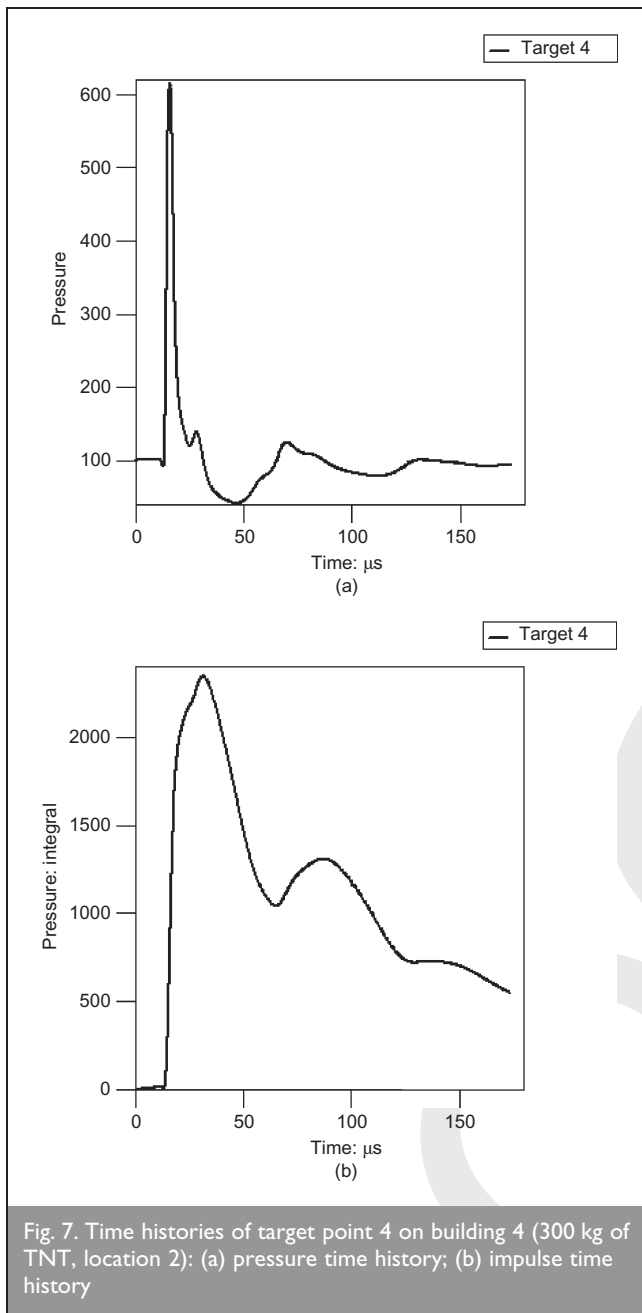


Fig. 7. Time histories of target point 4 on building 4 (300 kg of TNT, location 2): (a) pressure time history; (b) impulse time history

is dissipated in the process of destruction of structures and materials. However, according to numerical tests performed, and taking in account other tools used, such as isodamage curves, this simplification does not significantly affect the final results.

4. ISODAMAGE CURVES

When a blast wave encounters a solid surface the pressure is instantaneously modified owing to the reflection of the incident wave. Reflected pressure is a function of overpressure and dynamic pressure. In general, the peak value of the reflected overpressure depends on the intensity of the incident wave, the angle of incidence, and the stiffness of the object on which the pressure is reflected.

The assessment of damage due to explosive-produced loads on structures can be performed with modern computer codes.⁵

However, this would require the detailed discretisation of the buildings analysed, and could be prohibitive in terms of time

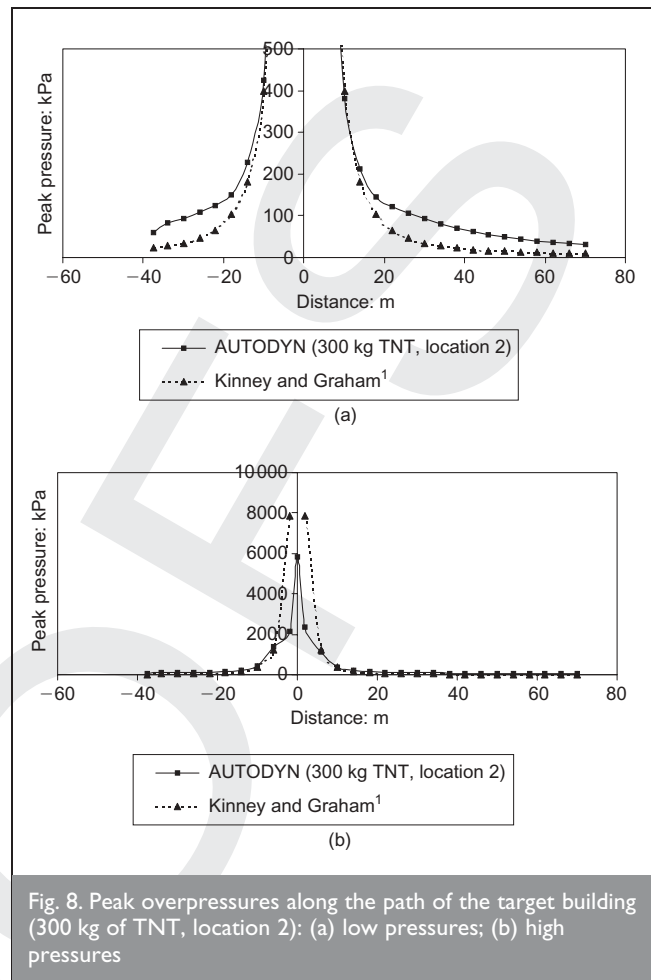


Fig. 8. Peak overpressures along the path of the target building (300 kg of TNT, location 2): (a) low pressures; (b) high pressures

and cost in the case of a complete block of buildings such as that considered in the present problem. Alternatively, the use of isodamage curves, which can be found in the literature,^{3,4,6,7} seems to be a more attractive way to relate pressures and impulses approximately to damage produced in different types of building and parts of them. In general, isodamage curves have been obtained from a wide compilation of data relating to damage produced in masonry houses and other buildings and structural elements in both experimental and actual explosions. The resulting diagrams are similar to those obtained theoretically for the ultimate load of single degree of freedom elastic systems when a maximum displacement is allowed.⁶

One of the diagrams used in this paper is that shown in Fig. 10(a), that was presented by Baker^{3,6,7} and relates different damage levels in brick-built houses to peak overpressure and impulse. The different damage levels defined in Fig. 10(a) correspond to:

- (a) zone A (above line B): almost complete demolition
- (b) line B: such severe damage as to require demolition; 50–70% of external brickwork destroyed or unsafe
- (c) line Cb: damage rendering house temporarily uninhabitable; partial collapse of roof and one or two external walls; load-bearing partitions severely damaged, requiring replacement
- (d) line Ca: relatively minor structural damage, yet sufficient to make house temporarily uninhabitable; partitions and joinery wrenched from fixings
- (e) zone D (below line Ca): damage calling for urgent repair,

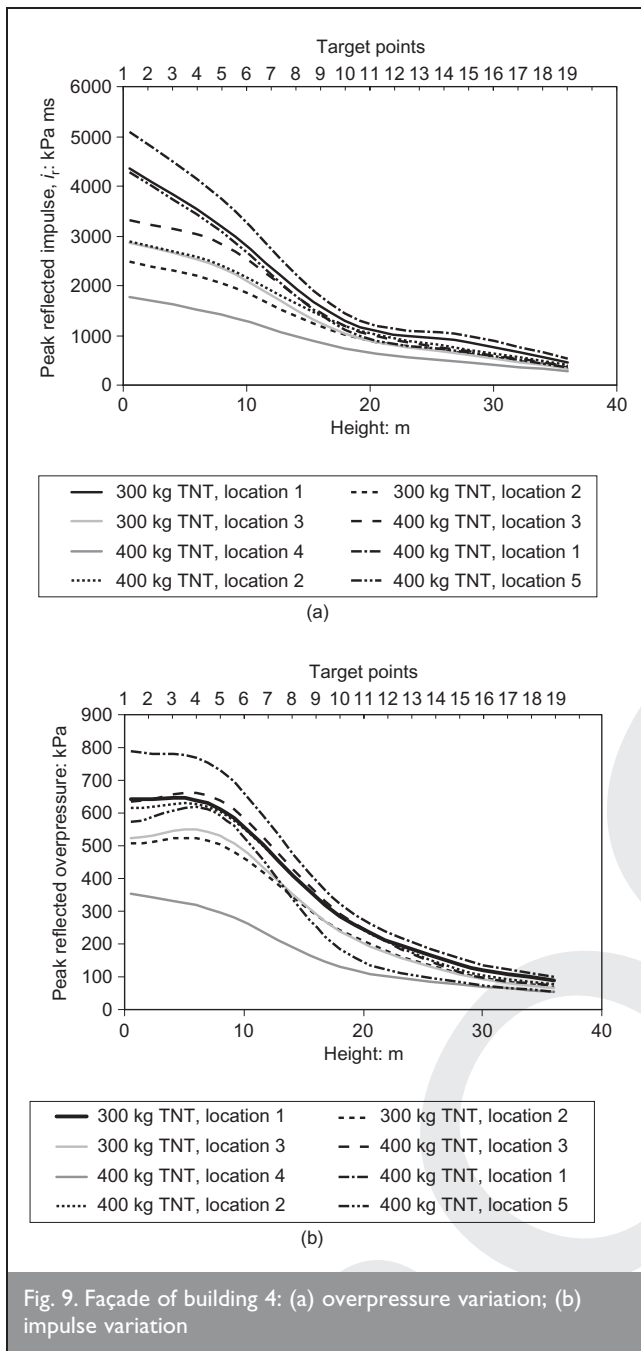


Fig. 9. Façade of building 4: (a) overpressure variation; (b) impulse variation

but not so as to make house uninhabitable; damage to ceilings and tiling; more than 10% of glazing broken.

These isodamage diagrams must be converted into diagrams relating reflected pressures and impulses to damage levels in order to use them to obtain the levels of damage corresponding to reflected values of pressure and impulse obtained in the numerical simulation. The resulting curves, which are obtained by using empirical expressions and charts,^{1,6,7} are presented in Fig. 10(b).

These diagrams define global levels of damage to assess safety and need for demolition, but do not make precise reference to the type of wall or structure affected by the explosion. As an alternative, the diagrams presented by Millington,⁴ which relate incident overpressure to distance for different masses of explosive and damage levels, were used. These curves, presented in Fig. 11(a), correspond to masses of explosive from

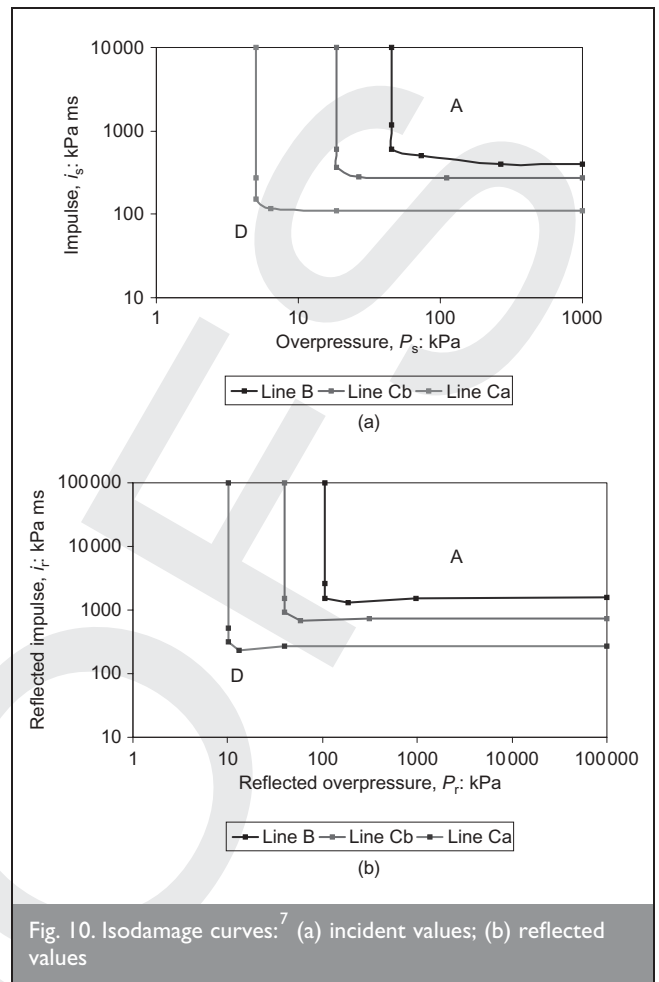


Fig. 10. Isodamage curves:⁷ (a) incident values; (b) reflected values

1 to 500 kg of TNT, and have a finer specification for damage levels in different types of structural and non-structural element. These diagrams were also converted into graphics relating reflected values of pressure and impulse to damage levels. The resultant curves are presented in Fig. 11(b).

In Fig. 12 both diagrams are presented, and it can be concluded that the limits are similar in both cases. The level of damage corresponding to total demolition^{3,6,7} in one case corresponds to the level of demolition of 250 mm and 100thk;mm walls in the other case.⁴

5. DAMAGE CONTOURS

In this section the results of the simulated pressure and impulses, obtained for some of the buildings and all the combinations analysed, are plotted on the isodamage diagrams. In fact, all the combinations and buildings should be analysed, but in this paper, because of limited space and for clarity reasons, only the results obtained for buildings 1 and 4 (Fig. 3) for 300 and 400 kg of TNT placed in various locations considered, are presented.

(a) *Building 1.* The numerically obtained peak reflected overpressures and impulses along a vertical line placed in the centre of the building façade and starting from 0.25 m above the soil are presented in Fig. 13 to allow comparison with the isodamage curves previously described. The values presented correspond to the target points indicated in Fig. 3(a). It can be observed that, as expected, the values of pressure and impulse decrease with height. In all cases, the

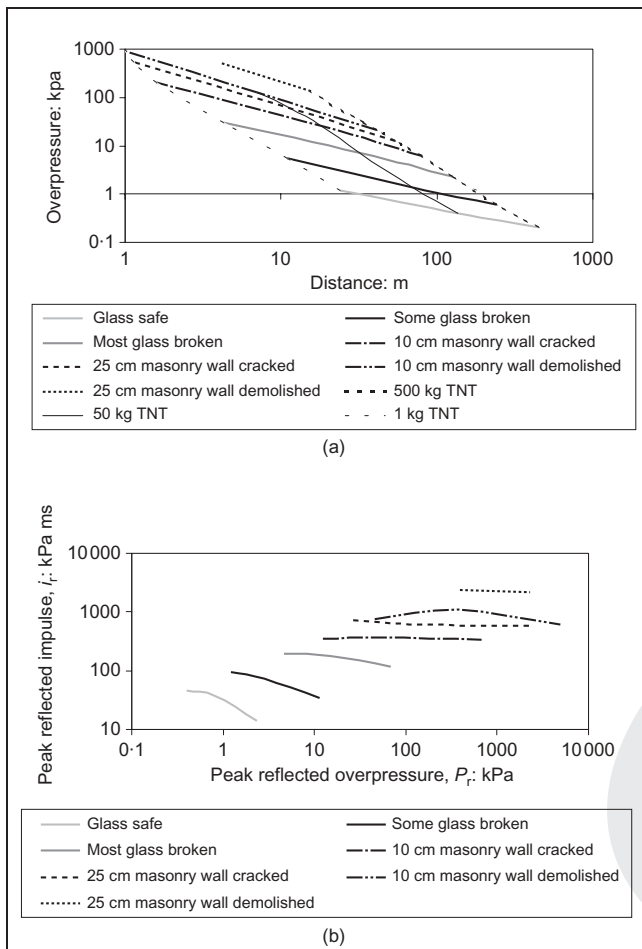


Fig. 11. Isodamage curves by Millington:⁴ (a) incident values; (b) reflected values

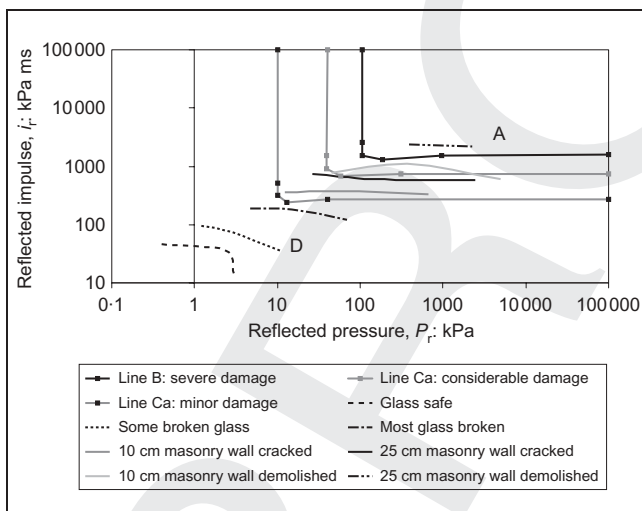


Fig. 12. Comparison of isodamage curves.

lower points of the façade of building 1 have values of pressure and impulses greater than the levels for total demolition.

(b) **Building 4.** The peak reflected overpressures and impulses obtained numerically along a vertical line placed in the centre of the building façade and starting from 0.25 m above the soil are presented in Fig. 14 for comparison with isodamage curves. The values presented correspond to the target points shown in Fig. 3(b). It can be seen that a

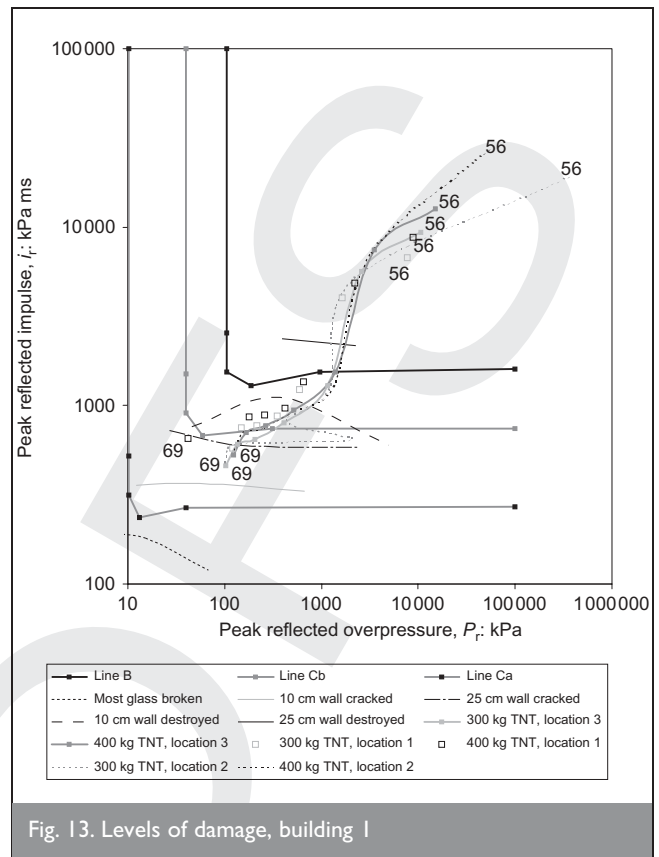


Fig. 13. Levels of damage, building 1

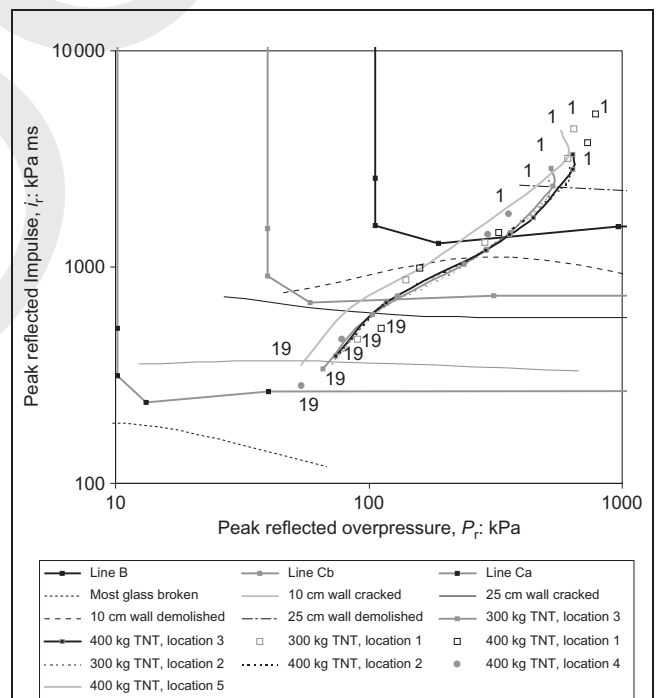


Fig. 14. Levels of damage, building 4

significant reduction in impulses is obtained for the case corresponding to the explosive located in the subsoil of the target building (location 4 in Fig. 4 and Table 1), as opposed to when it is located above the ground level.

It should be noted that according to Figs 13 and 14, for the range of explosive masses analysed, the level of damage is practically independent of the pressure value.

In this section, condensed charts or diagrams, called *damage contours*, with the different levels of damage spatially identified in the block of the target building, will be presented.

In order to construct these maps of isodamage, and taking into account the isodamage curves defined by other authors,^{3,4,6,7} the following numerical levels of reflected impulses were defined for different types of damage in structural and non structural-elements:

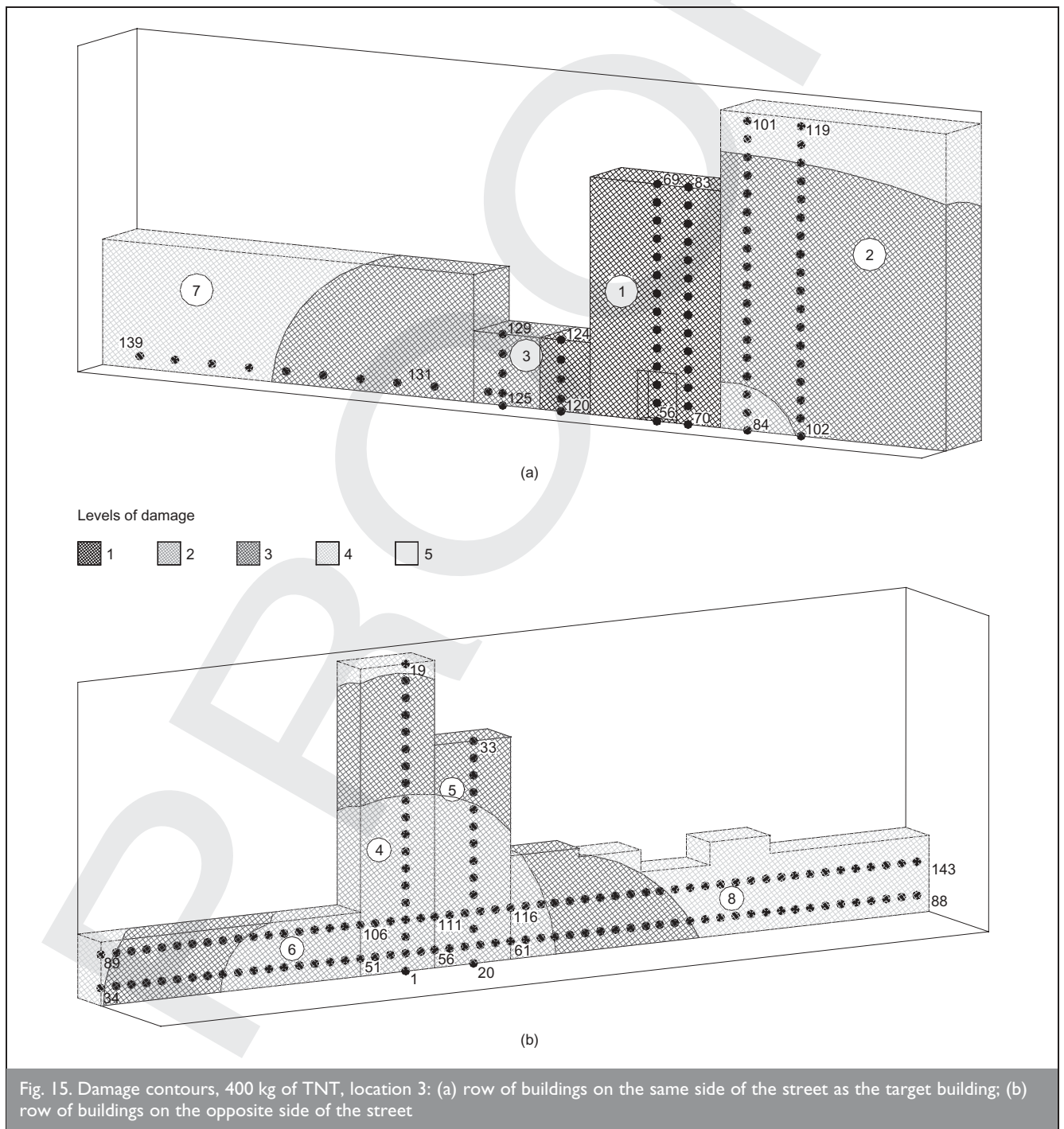
1. $i_r > 3000$ kPa ms (reinforced concrete structure destroyed)
2. 1000 kPa ms $< i_r < 3000$ kPa ms (masonry walls destroyed, reinforced concrete structure damaged)
3. 500 kPa ms $< i_r < 1000$ kPa ms (masonry walls cracked)
4. 180 kPa ms $< i_r < 500$ kPa ms (most glass destroyed; external joinery, ceiling and tiling damaged)




5. $i_r < 180$ kPa ms (some glass undamaged).

Moreover, in order to obtain coherent maps, the structural configuration (reinforced concrete structure or masonry structure) should also be taken into account. For example, if all the load-bearing structure in a lower stage is destroyed, then the upper stages should be considered destroyed too, although the levels of impulses were lower than the appropriate limit for the upper structure.

In correspondence with the numerical levels defined above, the following colour levels are defined:

-  1. total demolition
-  2. masonry walls destroyed, reinforced concrete structures damaged



-  3. masonry walls cracked
-  4. most glass destroyed; external joinery, ceiling and tiling damaged
-  5. some glass undamaged.

Again, for space reasons, only three combinations are presented. In Figs 15–17 the simulated maps of isodamage for 400 kg of TNT in locations 3, 4 and 5 (Fig. 4 and Table 1) are presented.

6. COMPARISON WITH REAL DAMAGE

The last step in the methodology presented above is comparison of the simulated damage contours with those obtained for real damage. This procedure leads to the discarding of most of the combinations considered at the beginning of the analysis.

It can be seen in Figs 15(b) and 17(b) that locations 3 and 5 do not produce damage that is significantly different in the row of buildings on the opposite side of the street, but the differences are appreciable in the row of buildings on the same side as the target building (Figs 15(a) and 17(a)). Comparison with the real damage presented in Fig. 3(a) makes it possible to discard the combination corresponding to Fig. 17.

Moreover, it can be seen in Figs 15(b) and 16 that locations 3 and 4 produce damage that is significantly different in the row of buildings on the opposite side of the street. In Fig. 16 it can be observed that part of the block on the opposite side of the street has some glass undamaged, which is a very significant reason for discarding the combination corresponding to this figure.

In this way, by analysing the damage contours obtained for all the combination of Table 1 and comparing them with the real damage presented in Figs 1–3, it can be concluded that, for

this case, the location of the explosive was that indicated in Fig. 18, and that the mass of explosive was between 300 and 400 kg of TNT.

7. CONCLUSIONS

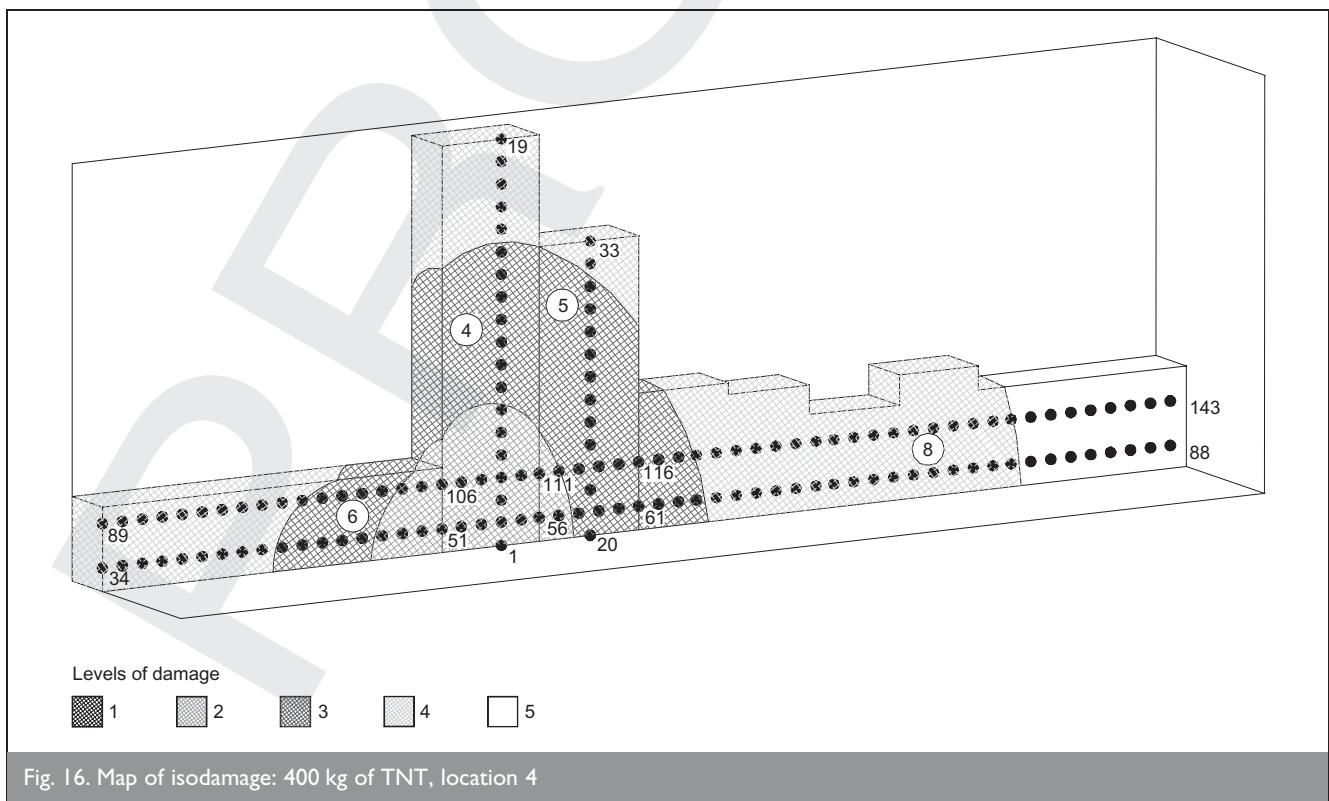
A numerical-computational methodology to assess the pressures and impulses generated by blast loading in structures is presented. The values obtained constitute an important issue for the design of structures to withstand the effects of blast loading, because better quantification of the effects should lead to more cost-effective design.

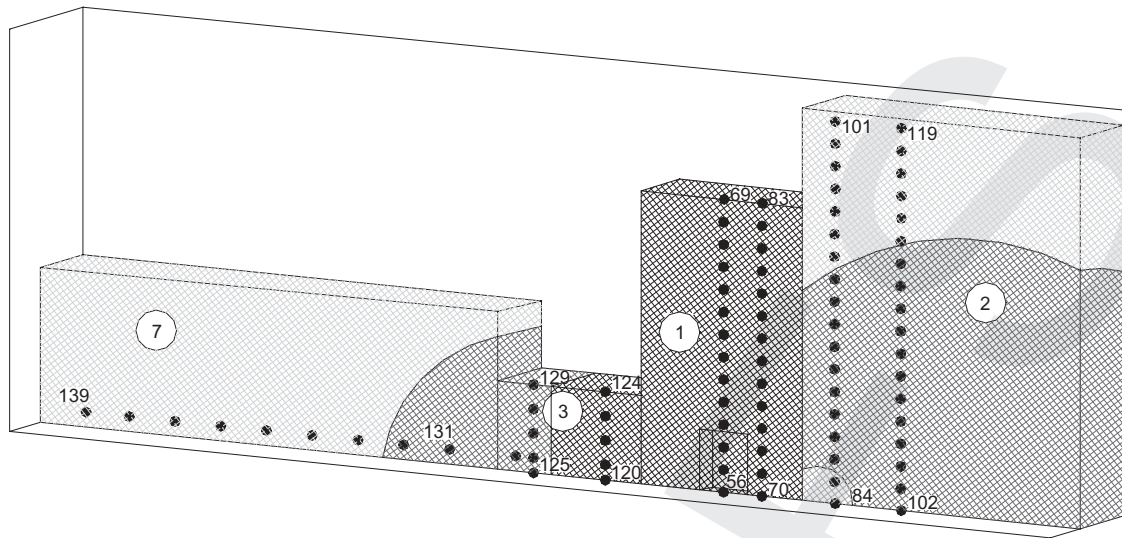
According to the results presented in the paper, it is clear that the use of empirical expressions is not sufficient for the accurate evaluation of incident pressure distributions and associated impulses in complex urban environments. Neglecting reflections and the ‘mach effect’ of the blast wave could lead to important underestimation of the peak values in the far field. Moreover, empirical expressions are not applicable with confidence in the near field because of the complexity of the flow processes involved in forming the blast wave.

A methodology to assess the correlation between pressure and impulse and the structural response, particularly the resulting global damage, is presented. Damage contours constitute an innovative approach to identifying zones with different types of damage.

The isodamage diagrams presented in this paper are in terms of reflected overpressures and impulses, and are useful for use by others because there is not enough information about this topic in the open literature.

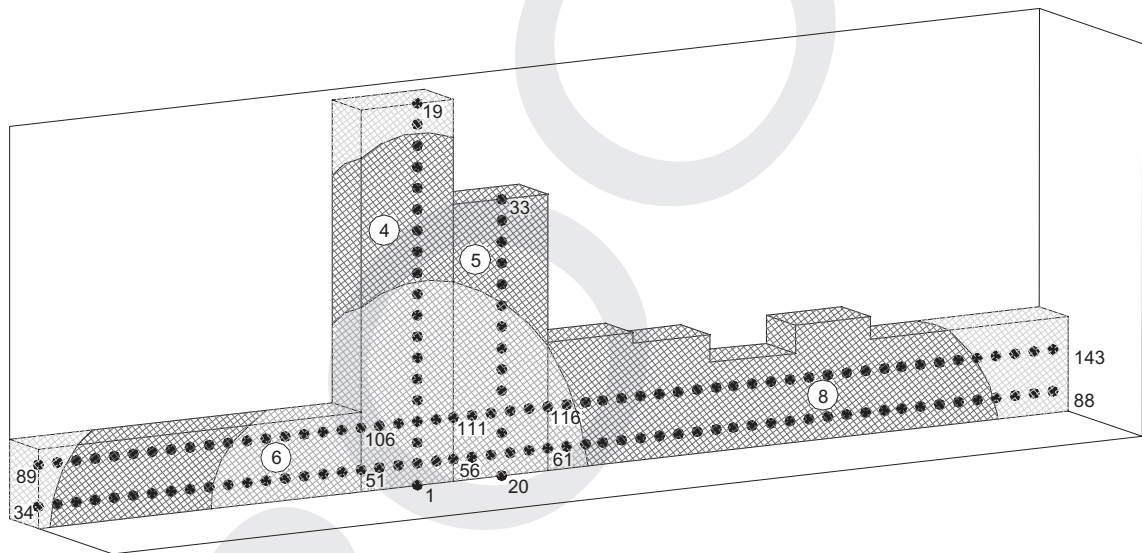
Comparison of the simulated damage contours with those obtained for real damage make it possible to discard most of the combinations of mass of explosive and location considered





(a)

Levels of damage



(b)

Fig. 17. Damage contours, 400 kg of TNT, location 5: (a) row of buildings on the same side of the street as the target building; (b) row of buildings on the opposite side of the street

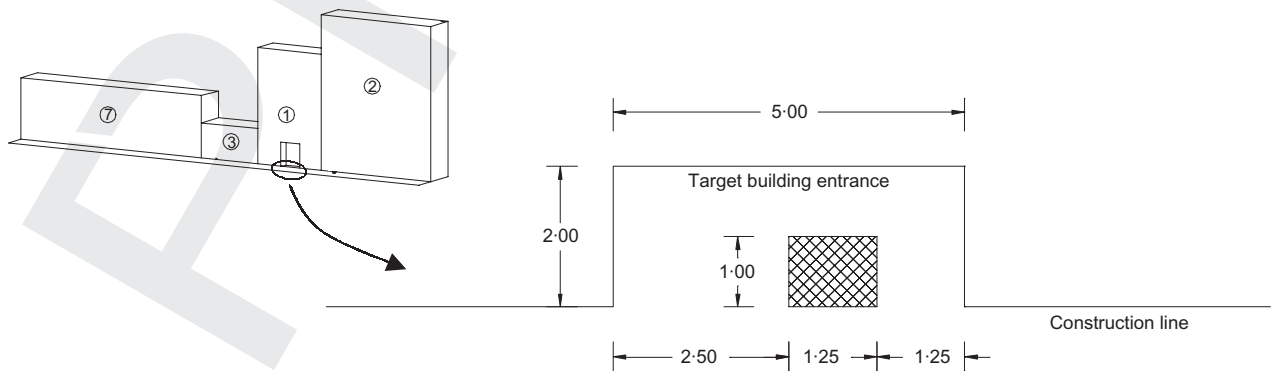


Fig. 18. Plan of the location of the origin of the explosion

at the beginning of the analysis, leading to the selection of the most probable and reliable combination.

It is important to note that, when the target building is destroyed by the explosion, damage in that building is not so sensitive to changes of mass and location of the explosion as damage to the façades of the buildings located in front of it.

The methodology for determining the location of the blast load in a terrorist attack, when there is not clear evidence of a crater, can be summarised in the following steps:

1. Detailed assessment of *actual damage*; construction of *actual damage* contours.
2. Definition of the limiting range of explosive mass that could have been used, and the limits of the widest zone where it might have been located. This step must be based on visual inspection of damage and analysis of particular features of the scenario analysed, such as traffic direction, which make some situations possible and others impossible.
3. Numerical evaluation of the pressures and impulses generated by blast load on the building façades located within the zone where damage is important, for the different combinations defined in the previous step. This step must be performed using appropriate numerical tools that allow consideration of multiple reflections of the blast wave, such as hydrocodes.
4. Estimation of damage corresponding to the calculated pressures and impulse using isodamage curves. Construction of *simulated damage* contours.
5. Comparison of actual and calculated damage contours.
6. Discarding of the possibilities for which *actual* and *simulated damage* contours are not coincident.
7. Determination of the most probable location and mass of

the explosive charge as those for which *actual* and *simulated damage* contours are similar.

8. ACKNOWLEDGEMENTS

The authors wish to acknowledge the collaboration of Eng. Sergio Gutiérrez and Abel Jacinto. The financial support of CONICET, the Universidad Nacional de Tucumán and Argentine Judiciary is gratefully acknowledged. Special acknowledgements are extended to Drs Bence Gerber and Chris X. Quan for technical support regarding the use of AUTODYN.

REFERENCES

1. KINNEY G. F. and GRAHAM K. J. *Explosive Shocks in Air*, 2nd edn. Springer, Berlin, 1985.
2. AMBROSINI R. D., LUCCIONI B. M., DANESI R. F., RIERA J. D. and ROCHA M. M. Size of craters produced by explosive charges on or above the ground surface. *Shock Waves*, Springer, Berlin (in press).
3. ELLIOTT C. L., MAYS G. C. and SMITH P. D. The protection of buildings against terrorism and disorder. *Proceedings of the Institution of Civil Engineers—Structures & Buildings*, 1992, **94**, 287–297.
4. MILLINGTON G. S. Discussion of 'The protection of buildings against terrorism and disorder' by C. L. Elliott, G. C. Mays and P. D. Smith. *Proceedings of the Institution of Civil Engineers—Structures & Buildings*, 1994, **104**, 343–346.
5. AUTODYN. Interactive Non-Linear Dynamic Analysis Software, Version 4.2, User's Manual, Century Dynamics Inc., 2001.
6. BAKER W. E., COX P. A., WESTINE P. S., KULESZ J. J. and STREHLOW R. A. *Explosion Hazards and Evaluation*. Elsevier, Amsterdam, 1983.
7. SMITH P. D. and HETHERINGTON J. G. *Blast and Ballistic Loading of Structures*, Butterworth-Heinemann, Oxford, 1994.

Please email, fax or post your discussion contributions to the secretary: email: mary.henderson@ice.org.uk; fax: +44 (0)20 665 2294; or post to Mary Henderson, Journals Department, Institution of Civil Engineers, 1–7 Great George Street, London SW1P 3AA.